Structure and Molecular Mobility at Free Surfaces of an *n*-Alkane Crystal: A Monte Carlo Simulation

Takashi Yamamoto*

Department of Physics, Faculty of Science, Yamaguchi University, Yamaguchi 753, Japan

Masamichi Hikosaka

Department of Material Science and Engineering, Faculty of Engineering, Yamagata University, Yonezawa 992, Japan

Nobuyuki Takahashi

Hokkaido University of Education, Hachiman-cho, Hakodate 040, Japan

*Received September 3, 1993; Revised Manuscript Received December 4, 1993**

ABSTRACT: Structures of typical low index surfaces, {100} and {110}, of an *n*-alkane crystallite made up of 400 molecules are investigated by Monte Carlo simulation. Each molecule in the crystallite is assumed to be rigid and to make rotation and translation about the chain axis as well as transverse displacement from the reference lattice point. The structure and molecular mobility at each surface, and their temperature dependence, are studied as a function of depth from the surface. In a fully ordered state at lower temperature, where the crystallite has the usual herringbone structure, the molecules near the surfaces also pack in a similar herringbone structure. The increase in temperature gives rise to very pronounced disorders at the surface regions of two or three molecular layers, especially at the {100} surface, besides overall disordering in the crystallite. The surface disorder is found to be characterized by the loss of the typical herringbone structure and the enhanced translation of the chain; these features are shown to be characteristic of the rotator phase RI of an *n*-alkane. The significance of such disordered surface structures in the crystal growth theory is discussed.

1. Introduction

The surface of the material is the forefront of most interactions with the surroundings. It is a subject of great interest in almost every branch of material science. For example, the surfaces of bulk polymers play crucial roles in adhesion, mixing, etc. Nowadays molecular simulations of the microscopic surface structures of amorphous polymers are also available.[1] Molecular simulation studies of crystal surfaces of polymers, on the other hand, are still very scarce.[2,3] The crystal surface is the main stage of crystal growth. The microscopic structure and the molecular mobility at the crystal surface, and their dependence on the surface index, are of great importance in understanding the nucleation and growth processes of polymer crystals.[4–6]

The purpose of the present paper is to investigate the static and dynamic structure of crystal surface of *n*-alkanes, model substances of polyethylene, and to reason out the significance of the detailed surface structure in the crystal growth.

We have hitherto performed various computed simulations, by both Monte Carlo (MC)[7–9] and Molecular dynamics (MD)[10,11] methods, of dynamical structures of crystalline polymers and alkanes. We here adopt our previous MC method used in the study of the rotator phases of *n*-alkanes.[9] We investigate the structures of typical low index surfaces of alkanes as functions of depth; thereby we hope to introduce a new point of view to the polymer crystallization theory. The detailed surface structure depends on temperature (a measure of molecular disorder) and lattice constants (measures of crystalline constraint); the lattice constants should be determined from temperature under a given constant pressure. In this short report, however, we neglect the effect of lattice dilatation and make a constant volume simulation; a preliminary MC study at constant pressure and temperature suggested that the volume change is fairly small within the present temperature range. Detailed simulations at constant pressure and temperature, by T–P ensemble Monte Carlo, will be carried out in a near future.

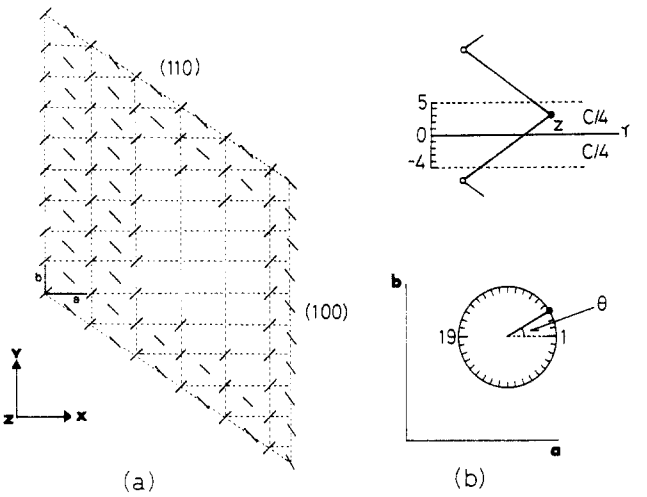

Figure 1. (a) Two-dimensional crystallite of an *n*-alkane surrounded by {100} and {110} surfaces. Ordinary orthorhombic unit cell of the reference lattice, with dimensions *a* and *b*, is also shown. (b) Molecular transition *z* and orientation θ are defined with respect to a reference plane, γ, and the crystal axis *a*, respectively. Both *z* and θ have discrete values, $z = (Cn)/20$ ($n = -4$ to 5) and $\theta = 10n°$ ($n = 0$ to 35).

2. Model and Calculation Method

The present model is similar to those used in our previous simulations of the rotator phases of *n*-alkanes.[9] We consider an *n*-alkane crystallite, 20×20 molecules in size, surrounded by {100} and {110} surfaces (Figure 1), where the surfaces are free and subjected to no extra boundary

* Abstract published in *Advance ACS Abstracts*, February 1, 1994.

0024-9297/94/2227-1466$04.50/0

conditions. As in our previous simulations, we here neglect the intramolecular degrees of freedom by assuming that the molecules are rigid planar zigzag with fixed bond lengths and bond angles: d(CC) = 1.54 Å, d(CH) = 1.09 Å, ∠CCC = 112°, ∠HCH = 110°.[9] We also neglect the chain end effects; the interchain energies per C_2H_4 segment are calculated. The rigid chain assumption, of course, fails when the chains are long and the flexibility cannot be ignored; we are here concerned with relatively short alkanes.

Consider a two-dimensional reference lattice of orthorhombic form a = 7.25 Å and b = 5.0 Å (Figure 1). We assume that each molecule is distributed around one of the lattice points and has the following degrees of freedom: rotation about the chain axis; translation along the chain axis, and transverse displacement from the lattice point. The rotation and translation of each chain are described by the direction θ and the height z of a carbon atom nearest to a reference plane, γ, where discrete 36 and 10 states are assumed for the former and the latter degrees of freedom (Figure 1); the transverse displacement of the chain takes continuous values within a limited range. Here we have to remark that the transverse displacements, if they are arbitrary in directions and magnitudes, give rise to a lattice instability specific to the two-dimensional system: the crystallite does not have positional long range order. Since we are here interested in a three-dimensional crystallite, we have introduced the reference lattice points from which each chain is considered to make random transverse displacements within a given range: 1 Å in the present calculation. Such imposed reference lattice constraint means that we are implicitly assuming some kind of interactions with a substrate, where the energies of these interactions should be sufficiently small to be neglected in the discussion of the structure within the layer.

We take into account the interactions between chains whose interaxial distances are less than 10 Å; the cutoff radius is 10 Å. For ease of comparison with our previous work,[9] we here use Williams set IV potentials[12] for the calculations of the van der Waals interactions between H–H, C–H, and C–C atoms. In our previous work,[9] the energies of every possible type of interactions were calculated beforehand and they were read out in every MC move. In the present model, however, the interchain distances vary continuously, and therefore it is not expedient to adopt the previous scheme of interchain energy calculation. Here in this work, the interchain energies are calculated in every MC move by use of a following accelerated calculation scheme. We first calculate each row interaction between a row of α atoms and a row of β atoms (α, β = C or H) as a function of distance r and relative translation z, ($\Phi_{CC}(r,z)$, $\Phi_{CH}(r,z)$, $\Phi_{HH}(r,z)$); then the interaction between A chain and B chain is reduced to the calculation of 36 row interactions between 6 rows (two C rows and four H rows) of A chain and 6 of B chain.

Calculations were made at three successive temperatures, 100 K, 150 K, and 200 K; the temperatures are scaled appropriately considering short alkane C_{10}. These three states will be found to correspond to a well-ordered, a slightly disordered, and a fully disordered, state, respectively. A MC calculation at the lowest temperature (100 K) was carried out first. The equilibrium state obtained by the MC calculation was used as an initial state for the next MC calculation at higher temperatures. At each temperature, the MC calculation of 2×10^4 MCS was made for equilibration; 10 samples during another 10^4 MCS were used for calculations of the statistical properties.

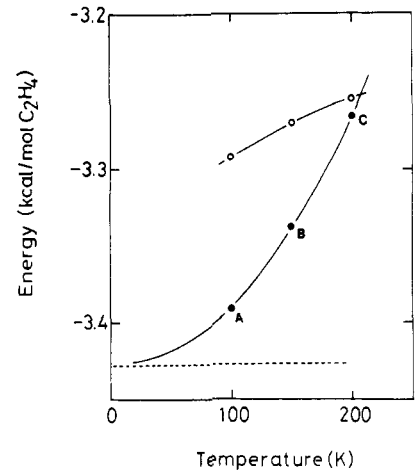

Figure 2. Equilibrium lattice energy vs temperature obtained after 3×10^4 MCS. Filled circles (●) are obtained from the ordered initial state, and open circles (○) are from the disordered initial state. The horizontal dotted line shows the energy level of the fully ordered state. The initial disordered state was found not to converge easily to the ordered state at lower temperatures.

The initial state used in the MC calculation at 100 K had a perfectly ordered heringbone packing with no translational and transverse disorders. It was found that highly disordered initial states do not easily converge to the ordered states at lower temperatures (Figure 2); the positional disorder as well as the orientational disorder persist for a fairly long time. This is probably because the transverse displacement (or the interchain separation) and the chain orientation are strongly coupled.[9]

3. Results

3.1. Average Structures. Before discussing detailed surface structures, we examine the overall structural changes with temperature. Increased thermal energy at higher temperatures leads to enhanced disorder in the crystal. Figure 2 shows that the lattice energy markedly increases above around 150 K; three successive states, at 100 K, 150 K, and 200 K, are hereafter abbreviated as A, B, C states, respectively. Corresponding structural changes are best exemplified in the distribution of the chain orientations (Figure 3). At 100 K, it has a two-site distribution, centered around θ = 40° and θ = 320°, characteristic of the ordered herringbone structure of polyethylene. With increasing temperature, both rotational and translational motions of the molecules become activated. At 150 K, we can readily notice a growth of the population at $\theta = 180 \pm 40°$. It represents π or $\pi/2$ rotations of the molecules from the original orientations; it should be remembered that π rotation is equivalent to $C/2$ translation from the 2_1 symmetry of the molecules. At the highest temperature, 200 K, we have finally a four-site distribution. The four-site distribution is known to be characteristic of the rotator phase I (RI phase)[13] (or FCO phase[14]) of orthorhombic symmetry;[9,15,16] though the phase is named rotator, the discrete four-site orientation in the RI phase was one of the major findings of recent computer simulations.[9,15]

Molecular translation along the axis also strongly depend on temperature. Figure 4 shows distributions of the chain translation z vs temperature. Even at the lowest temperature A, the translational disorder is readily appreciable. At the highest temperature C, the distribution becomes nearly uniform, indicating full disorder in translation. The onset of disorder at lower temperatures and fairly large disorder at higher temperatures are the main characteristics of the translational motion of the poly-

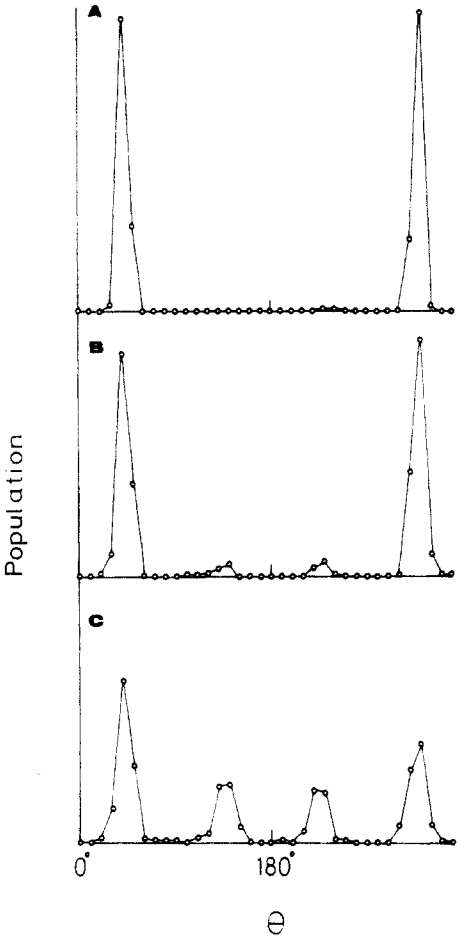

Figure 3. Orientation distributions averaged over the whole crystallite at three successive temperatures: A at 100 K, B at 150 K, and C at 200 K.

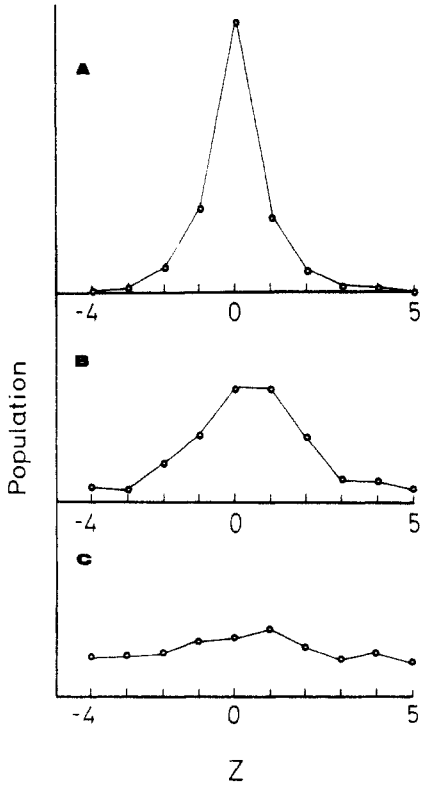

Figure 4. Translation distributions averaged over the whole crystallite at three successive temperatures: A at 100 K, B at 150 K, and C at 200 K.

methylene chains already noticed in previous simulations.[9,15-18] It should be remembered however that in real alkane systems the translational disorder will be restricted by the interlamella interactions, especially at lower temperatures.

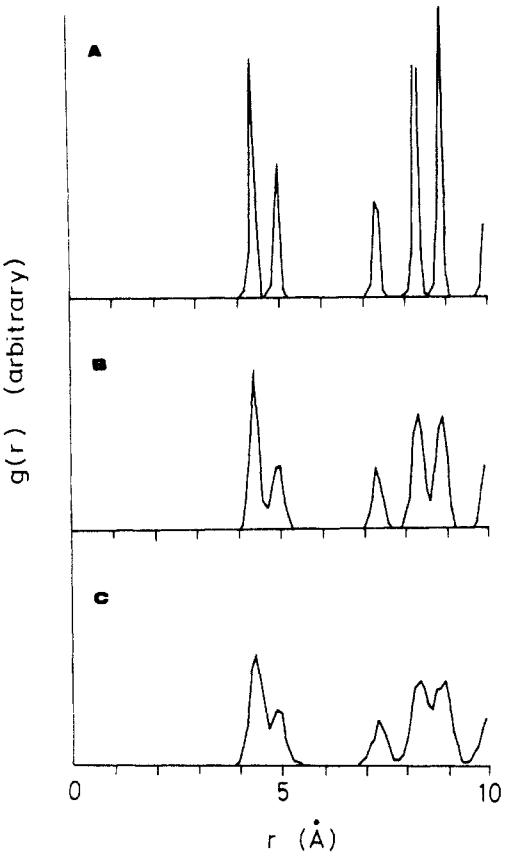

Figure 5. Two-dimensional radial distribution functions of the molecular axes at three successive temperatures: A at 100 K, B at 150 K, and C at 200 K.

The molecules at higher temperatures show large transverse displacements from the reference lattice points. Figure 5 shows the two-dimensional radial distribution functions of the molecular axes. The widths of the peaks markedly broaden with temperature, showing increased displacements at higher temperatures.

3.2. Surface Structures. Two-dimensional pictures of the crystallite, at B and C states, are given in Figure 6. The lateral positions and the orientations of the chains are expressed by the circles and the diametrical lines. At the lower temperature B, the chain orientations are those of well-known herringbone structure, in which the chains neighboring in ⟨110⟩ directions are mutually perpendicular. However considerable deviations from the ordered herringbone structure are observed near the {100} surfaces, where the chains are often parallel with each other. At the highest temperature C, the orientation of the whole system changes greatly to become a mixture of parallel and herringbone packings, a structure already found in our previous simulations of the rotator phase of *n*-alkanes.[9] Furthermore it is readily noticed, for both B and C states, that the positional disorder is very conspicuous at the first layers of the {100} surfaces.

The increased disorder near the surfaces has thus been clearly demonstrated. We now investigate the surface disorder in detail as a function of depth from the surfaces. We begin with the chain orientation. Figure 7 shows the distribution functions for the chain orientations on several molecular layers, both along {100} and {110} surfaces, of different depths d. The distribution functions are generally broader at the outermost surfaces $d = 0$ (0th molecular layer) than in the interior, especially for {100}

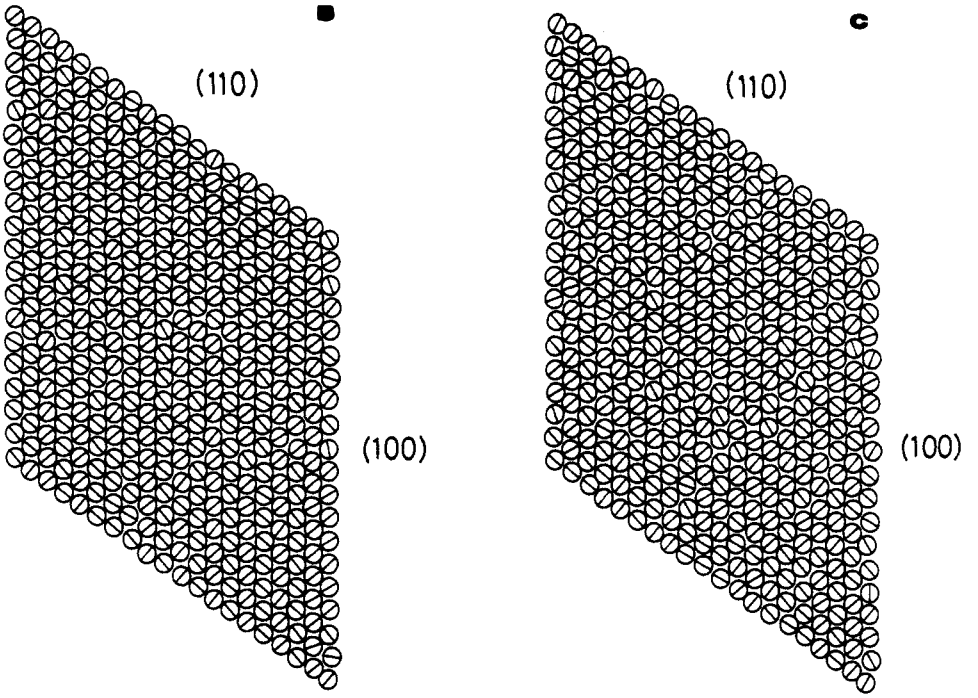

Figure 6. Two-dimensional pictures of the crystallite at 150 K (B) and 200 K (C). Positions of the molecules and the orientations are represented by the circles and the diametrical lines.

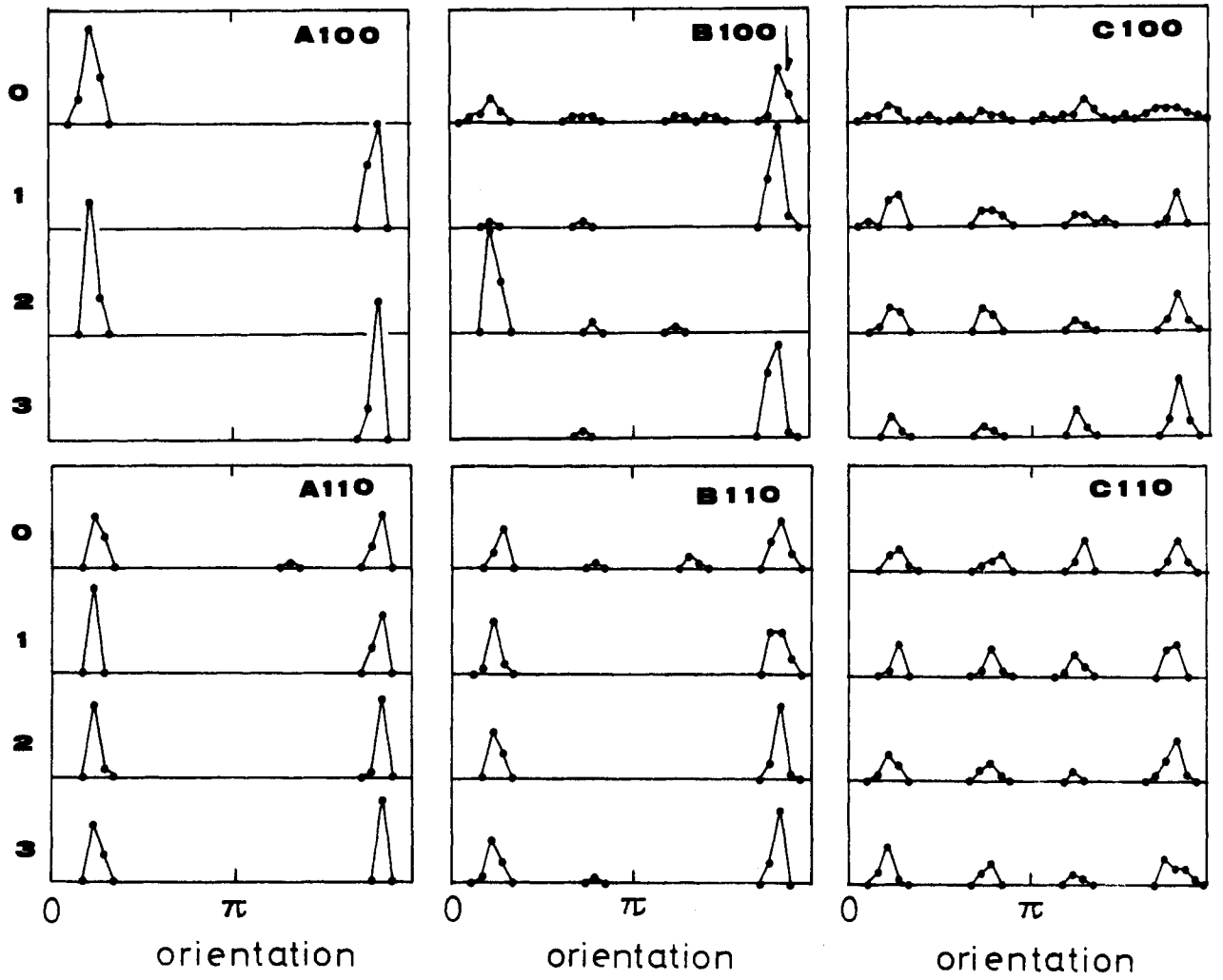

Figure 7. Distribution functions of chain orientations on each surface layer, of depth d (d = 0 to 3), of {100} (upper figures) and {110} (lower figures) surfaces, at (A) 100 K, (B) 150 K, and (C) 200 K.

surfaces. Molecular misorientation (arrow) is also observed at 0th layer in the B state. At the highest temperature C, {100} surfaces are very disordered, having nearly uniform orientation distribution. However, such highly disordered structures at the surfaces are quickly lost within a two or three molecular layer depth.

To be quantitative, we define the orientational short range order parameters from the cosine of setting angle

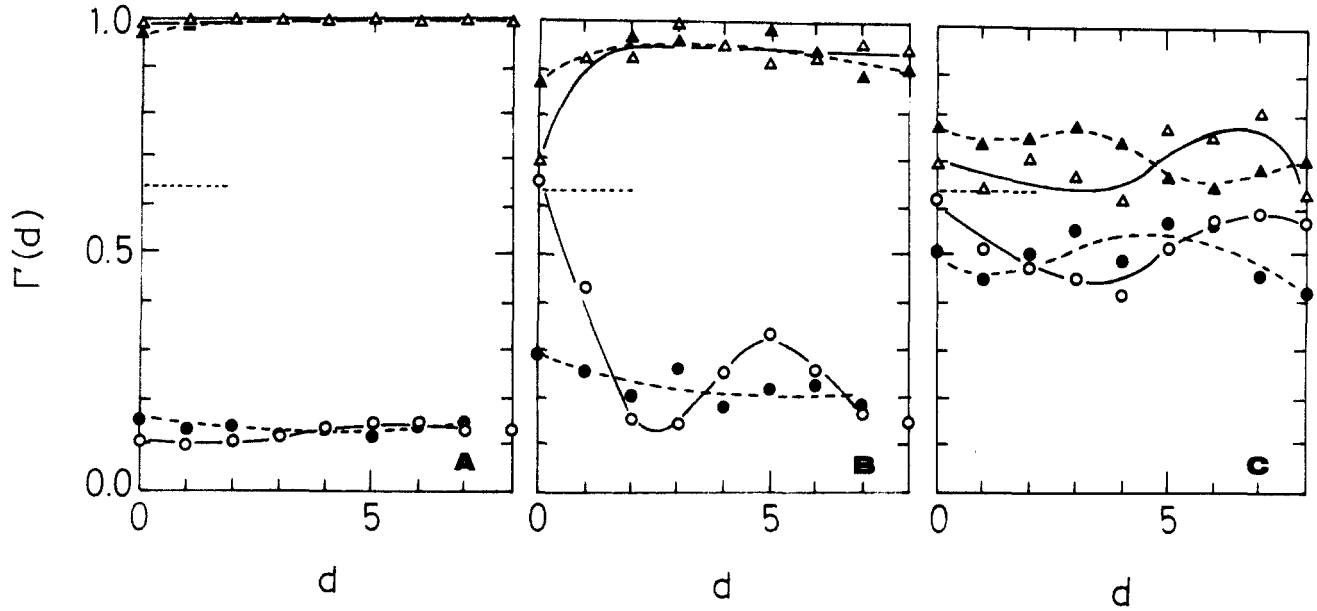

Figure 8. Short range order parameters for the chain orientations $\Gamma(d)$ vs depth d, in diagonal directions (●, ○) and in b axis (▲, △) directions. The open symbols (○, △) are those for {100} surfaces and the filled symbols (●, ▲) are those for {110} surfaces. Horizontal dotted lines are at $\Gamma = 0.637$, representing the fully disordered level of random orientations. Solid and dotted lines connecting open and filled symbols, respectively, are drawn only for the guide of the eye.

difference between neighboring chains. In the ordered state, the adjacent chains in b axis directions are strictly parallel, whereas those in diagonal directions are nearly perpendicular. We therefore take separate averages, giving order parameters $\Gamma_D(d)$ in the diagonal direction and $\Gamma_B(d)$ in the b axis direction, both as a function of depth.

$$\Gamma_D(d) = \langle|\cos(\theta(x,y) - \theta(x',y'))|\rangle;\ x' = x \pm 1,\ y' = y \pm 1 \quad (1)$$

$$\Gamma_B(d) = \langle|\cos(\theta(x,y) - \theta(x'',y''))|\rangle;\ x'' = x,\ y'' = y \pm 1 \quad (2)$$

where $\theta(x,y)$ is the orientation angle of the chain at sites (x,y), (x',y'), and (x'',y'') and represents respectively the sites in diagonal and b axis neighbors of (x,y). The averages are made over molecules at (x,y) on two layers of depth d from both side surfaces as well as over four neighboring chains in eq 1 or two in eq 2. No distinction is made here between parallel and antiparallel orientations of the chains. Figure 8 shows the changes in the order parameters for both {100} and {110} surfaces. At the lowest temperature A, the system has a fully ordered herringbone structure, and the orientation angles are about 40° and 320°. The order parameters Γ_D and Γ_B have therefore the corresponding ordered values $\Gamma_D \simeq 0.14$ and $\Gamma_B \simeq 1.0$ irrespective of d. At the higher temperature B, both Γ_D and Γ_B show considerable departures from those of the ordered state, especially near the surfaces. The surface disordering is much larger on {100} surfaces than on {110}; at the outermost {100} surface, both Γ_D and Γ_B are around 0.637, which is the value for the disordered limit. These features in Γ are in good accord with the disordered mixture of parallel and herringbone packings previously found near the {100} surfaces (Figure 6). Such disordered packings are, however, seen only in narrow regions of two or three molecular layer thicknesses. At the highest temperature C, the overall disorder in the bulk becomes very large, and the differences in the order parameters between the inner and the surface regions are no longer conspicuous.

Chain translation along the axis is also examined by use of a similar order parameter. The translation $C/2$ only replaces the z level of two carbons in C_2H_4, and these two states are here considered translationally equivalent. Taking the periodicity of $C/2$, we define the order parameter as follows.

$$\Lambda(d) = \langle|\cos(2\pi(z(x,y) - z(x',y'))/C)|\rangle \quad (3)$$

where $z(x,y)$ represents the translation of the chain at (x,y), C is the fiber period 2.55 Å, and the average is made over six neighboring chains (x',y') as well as over molecules on the molecular layers of depth d. Increased disorders are again seen near the surfaces {100} and {110} (Figure 9), but they are not so dependent on the surface index. The recovery of order in deeper layers is completed within two or three molecular layers.

The transverse disorder of the molecular axes was shown to increase considerably with increasing temperature (Figure 5). Lastly we calculated, as a function of depth, the average square displacement $\langle r^2\rangle$ of the chain axes from their mean positions (Figure 10). The molecules on the outermost surfaces show considerable transverse fluctuations. At the higher temperatures B and C, the increases in $\langle r^2\rangle$ at the surfaces are fairly abrupt, especially on {100} surfaces.

4. Summary and Discussion

All the results obtained in this simulation showed the presence of disordered surface regions of a two or three molecular layer thickness; the thickness is of order of 10 Å. The disordered structure at the surface is characterized by the loss of the typical herringbone (perpendicular) structure observed in the bulk and the enhanced chain translation; such a disordered structure was found to be characteristic of the rotator phase RI of n-alkanes. The disorder is especially pronounced on the {100} surface.

We have studied a cluster model of a short n-alkane. The model is simplified in many respects. First, all the chains are assumed to be rigid. However, the conformation of the chains near the surface may considerably deviate from the planar zigzag since the intermolecular constraints there are very weak. Second, the model is essentially two dimensional, and the long range positional order of the chain axes was artificially imposed by the reference lattice constraint. Nevertheless, we think this simplified model is a good starting model and is suitable to the investigation

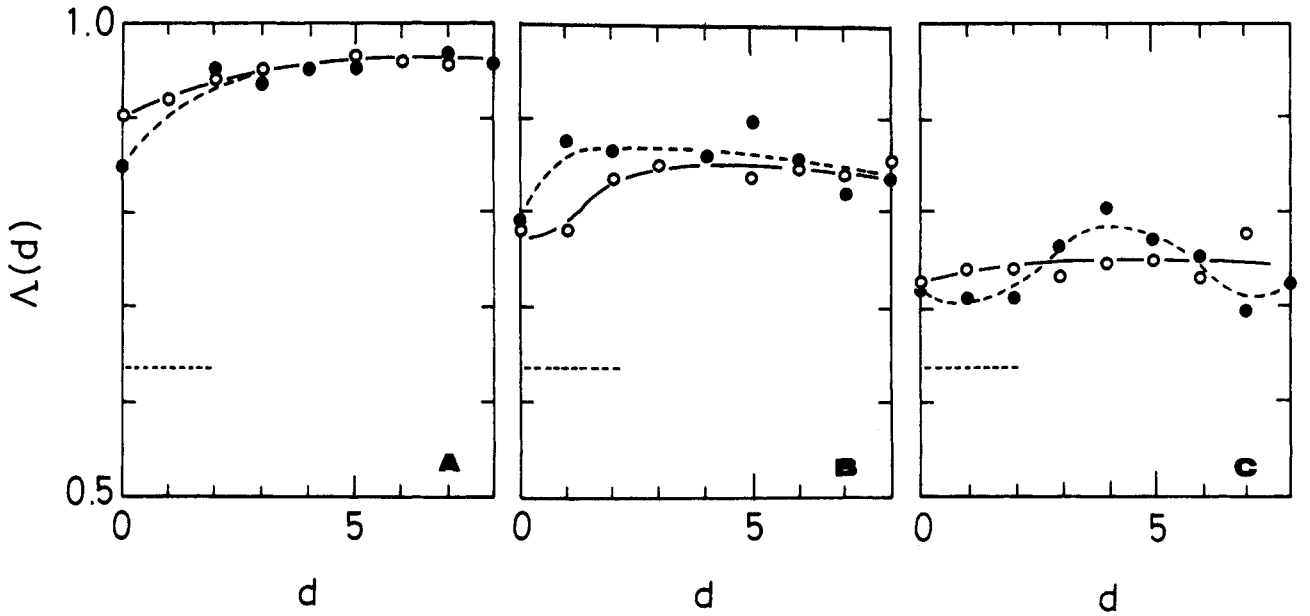

Figure 9. Short range order parameters for the chain translations $\Lambda(d)$ vs depth d. The open symbols (○) are those for {100} surfaces and the filled symbols (●) are those for {110} surfaces. Horizontal dotted lines are at $\Lambda = 0.637$, representing the fully disordered level of random translations. Solid and dotted lines connecting open and filled symbols, respectively, are drawn only for the guide of the eye.

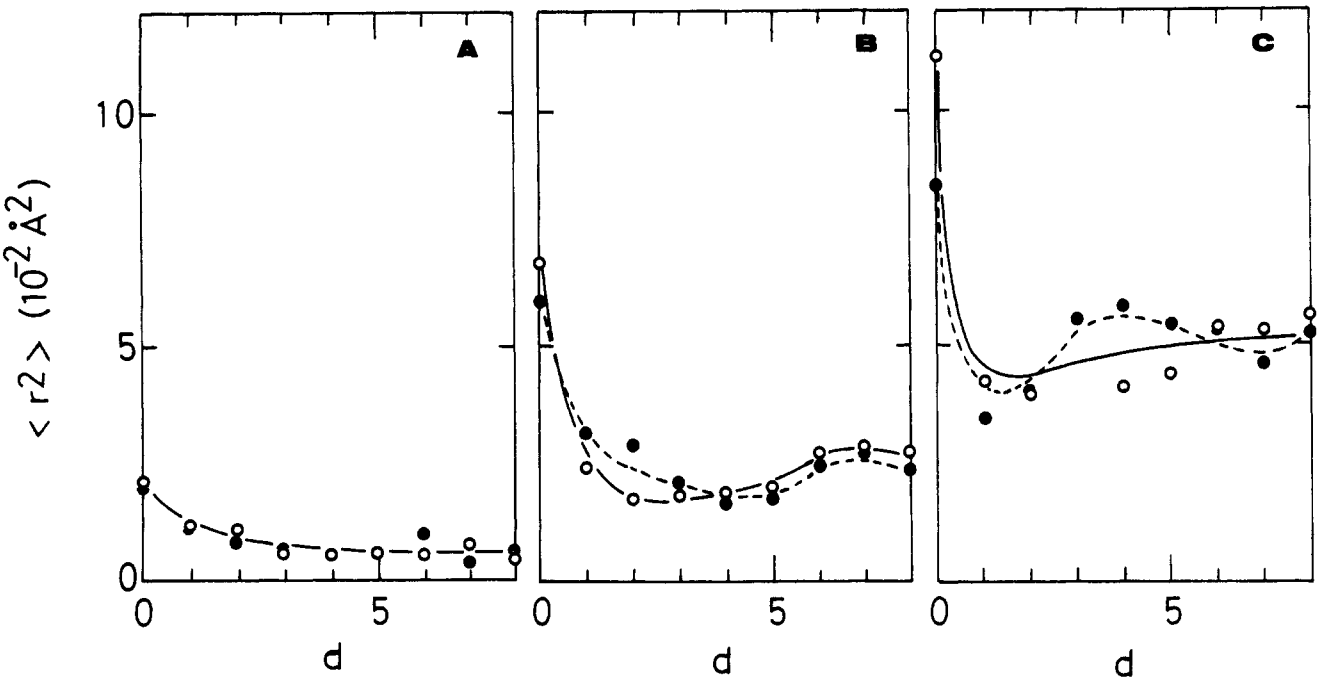

Figure 10. Averaged transverse fluctuations of the chain axis $\langle r^2 \rangle$ vs depth d for {100} (○) and {1$\bar{1}$0} (●) surfaces. Solid and dotted lines connecting open and filled symbols, respectively, are drawn only for the guide of the eye.

of the crystal growth process. We are now planning to extend the calculation of the attaching and detaching processes of molecules at the surfaces as well as surface structural reconstructions and thereby to simulate the nucleation and growth processes of n-alkane crystals. The significance of the characteistic surface properties obtained in the present work—the surface disorder or roughness, the chain mobility near the surfaces, and their dependence on the surface index—will be clarified in our future work. The surface structure and the chain mobility are important keywords, though not fully appreciated, in the understanding of crystallization. They will crucially control the nucleation and growth process of the crystal, as has been discussed by one of the authors.[6]

The discussion so far has been concerned with short alkanes for which the rigid chain assumption is valid. We here comment on the relevance to longer alkanes and polyethylene. We here considered C_{10} and assumed the chains are rigid. As long as the rigid chain assumption is valid, the interchain interactions are proportional to the chain length. The simulation of chains n times longer can be made by multiplying every interchain energy by n, or by dividing temperature by n; remember that temperature and energy always appear as the ratio in the Boltzmann factor. We think the rigid chain assumption is sound up to about C_{20}.

For longer chains, the chain twisting or the conformational defects of the molecules cannot be ignored. However, the defects are localized and the twisting is rather gradual;[10] they do not seriously disturb the chain packing. Therefore, as far as the local crystalline structure in the bulk is concerned, the requirement for the good packing of the hydrocarbon chains is the dominant structure determining factor. The structures obtained in our present

calculation are considered to be representative of the local structures of crystals of longer alkanes and polyethylene.

The surface structures are, on the other hand, considered to be quite different. The molecular conformation at the surface will considerably deviate from the ordered planar structure, and the chain connectivity will have a larger influence at the surface than in the bulk. We are also planning to investigate such surface structures of longer *n*-alkanes and polymers.

Acknowledgment. One of the authors (T.Y.) acknowledges the financial support from the Watanabe memorial foundation. He also appreciates the provision of the computing facilities from the Computer Center, Institute for Molecular Science, Okazaki National Research Institutes.

References and Notes

(1) Mansfield, K. F.; Theodorou, D. N. *Macromolecules* **1990**, *23*, 4430; **1991**, *24*, 6283.
(2) Patel, A. K.; Farmer, B. L. *Polymer* **1980**, *21*, 153.
(3) Liang, G. L.; Noid, D. W.; Sumpter, B. G.; Wunderlich, B. *Makromol. Chem., Theory Simul.* **1993**, *2*, 245.
(4) Phillips, P. J. *Rep. Prog. Phys.* **1990**, *53*, 549.
(5) Toda, A. *Polymer* **1991**, *32*, 771.
(6) Hikosaka, M. *Polymer* **1990**, *31*, 458.
(7) Yamamoto, T. *Polymer* **1983**, *24*, 943; **1984**, *25*, 178.
(8) Yamamoto, T. *J. Polym. Sci.; Polym. Phys. Ed.* **1985**, *23*, 771; *Polymer* **1986**, *27*, 986.
(9) Yamamoto, T. *J. Chem. Phys.* **1985**, *82*, 3790; **1988**, *89*, 2356.
(10) Yamamoto, T.; Kimikawa, Y. *J. Chem. Phys.* **1992**, *97*, 5163; **1993**, *99*, 6126.
(11) Takahashi, N. *Computer Aided Innovation of new materials II*; Doyama, M., et al., Eds.; Elsevier: Amsterdam, 1993; p 299.
(12) Williams, D. E. *J. Chem. Phys.* **1967**, *47*, 4680.
(13) Doucet, J.; Denicolo, I.; Craievich, A. F. *J. Chem. Phys.* **1981**, *75*, 1523.
(14) Ungar, G. *J. Phys. Chem.* **1983**, *87*, 689.
(15) Ryckaert, J. P.; Klein, M. L. *J. Chem. Phys.* **1986**, *85*, 1613.
(16) Ryckaert, J. P.; Klein, M. L.; MacDonald, I. R. *Phys. Rev. Lett.* **1987**, *58*, 698; *Molecular Physics* **1989**, *67*, 957.
(17) Noid, D. W.; Sumpter, B. G.; Wunderlich, B. *Macromolecules* **1990**, *23*, 664; **1991**, *24*, 4148.
(18) Sumpter, B. G.; Noid, D. W.; Wunderlich, B. *J. Chem. Phys.* **1990**, *93*, 6875.